


The P429L loss of function mutation of the human glycine transporter 2 associated with hyperekplexia

Alexandra Kitzenmaier¹ | Natascha Schaefer¹ | Vikram Babu Kasaragod² |
 Tilman Polster³ | Ralph Hantschmann⁴ | Hermann Schindelin² | Carmen Villmann¹ 

¹Institute for Clinical Neurobiology, Julius-Maximilians-University of Würzburg, Würzburg, Germany

²Rudolf Virchow Centre for Experimental Biomedicine, Julius-Maximilians-University of Würzburg, Würzburg, Germany

³Pediatric Epileptology, Mara Hospital, Bethel Epilepsy Centre, Bielefeld, Germany

⁴Center for Developmental Pediatrics and Pediatric Neurology, Hagen, Germany

Correspondence

Carmen Villmann, Institute for Clinical Neurobiology, Julius-Maximilians-University of Würzburg, Versbacherstr. 5, D-97078 Würzburg, Germany.
 Email: Villmann_C@ukw.de

Funding information

Deutsche Forschungsgemeinschaft, Grant/Award Number: VI586; Julius-Maximilians-University Würzburg

The peer review history for this article is available at <https://publons.com/publon/10.1111/EJN.14533>

Abstract

Glycine transporter 2 (GlyT2) mutations across the entire sequence have been shown to represent the presynaptic component of the neurological disease hyperekplexia. Dominant, recessive and compound heterozygous mutations have been identified, most of them leading to impaired glycine uptake. Here, we identified a novel loss of function mutation of the GlyT2 resulting from an amino acid exchange of proline 429 to leucine in a family with both parents being heterozygous carriers. A homozygous child suffered from severe neuromotor deficits. We characterised the GlyT2^{P429L} variant at the molecular, cellular and protein level. Functionality was determined by glycine uptake assays. Homology modelling revealed that the mutation localises to α -helix 5, presumably disrupting the integrity of this α -helix. GlyT2^{P429L} shows protein trafficking through various intracellular compartments to the cellular surface. However, the protein expression at the whole cell level was significantly reduced. Although present at the cellular surface, GlyT2^{P429L} demonstrated a loss of protein function. Coexpression of the mutant with the wild-type protein, reflecting the situation in the parents, did not affect transporter function, thus explaining their non-symptomatic phenotype. Nevertheless, when the mutant was expressed in excess compared with the wild-type protein, glycine uptake was significantly reduced. Thus, these data demonstrate that the proline residue at position 429 is structurally important for the correct formation of α -helix 5. The failure in functionality of the mutated GlyT2 is most probably due to structural changes localised in close proximity to the sodium-binding site of the transporter.

KEYWORDS

glycine transporter 2, glycine uptake, loss of function, presynaptic hyperekplexia, protein transport, structural disruption

Abbreviations: SLC, solute carrier; GlyT2, glycine transporter 2; ECD, extracellular domain; TM, transmembrane domain.

Edited by: Jochen Roeper.

This is an open access article under the terms of the Creative Commons Attribution License, which permits use, distribution and reproduction in any medium, provided the original work is properly cited.

© 2019 The Authors. *European Journal of Neuroscience* published by Federation of European Neuroscience Societies and John Wiley & Sons Ltd.

1 | INTRODUCTION

Glycine transporter 2 (GlyT2) is a sodium/chloride-dependent glycine transporter mainly located in presynaptic membranes of spinal cord and brainstem interneurons (Chalphin & Saha, 2010). GlyT2 is crucial for the transport of glycine from the synaptic cleft back into the presynaptic compartment where the neurotransmitter glycine will be packaged by the vesicular inhibitory amino acid transporter (VIAAT) into synaptic vesicles for a second release (Eulenburg, Arnsen, Betz, & Gomeza, 2005; Harvey, Topf, Harvey, & Rees, 2008).

Mutations in the *SLC6A5* gene encoding GlyT2 have been associated with the neuromotor disorder startle disease (hyperekplexia, stiff baby syndrome, OMIM 149400) (Carta et al., 2012; Eulenburg et al., 2005, 2006; Harvey et al., 2008; Masri, Chung, & Rees, 2017; Rees et al., 2006). Mutations in the *GLRA1* gene encoding the postsynaptic glycine receptor $\alpha 1$ are the major cause for startle disease, however, *SLC6A5* mutations are the second most common cause for this rare disorder (OMIM 604159) (Bode & Lynch, 2014; Schaefer, Roemer, Janzen, & Villmann, 2018). Symptoms of startle disease are stiffness in infancy, rigidity and enhanced startle reactions following an acoustic or tactile stimulus. Affected human individuals harbouring a mutation in the GlyT2 suffer from fatal apnoea episodes resembling sudden infant death syndrome (SIDS) (Nigro & Lim, 1992; Thomas et al., 2013; Vigeveno, Di Capua, & Dalla Bernardina, 1989). It was further demonstrated that a blockade of glycinergic inhibition generates failures in the respiratory rhythm (Busselberg, Bischoff, Paton, & Richter, 2001; Hulsmann et al., 2019; Shevtsova et al., 2014). In rodents, the GlyT2 knockout results in a similar phenotype compared with the human situation with lethality of homozygous knockout mice 3 weeks after birth (Gomeza et al., 2003).

Two classes of glycine transporters exist, GlyT1 and GlyT2, which are suitable therapeutic targets for the treatment of central and peripheral nervous system disorders (Harvey & Yee, 2013). The activities of both transporters depend on the concentrations of extracellular glycine, Na^+ and Cl^- ions. In contrast to GlyT1 which has a 2 Na^+ /1 Cl^- /glycine stoichiometry, GlyT2 exhibits a 3 Na^+ /1 Cl^- /glycine stoichiometry (Perez-Siles et al., 2012; Roux & Supplisson, 2000; Supplisson & Roux, 2002). The GlyT1 is mainly localised at astrocytes of the caudal CNS regulating the availability of glycine as a coagonist for the NMDA receptor (Zafra et al., 1995). In contrast, GlyT2 is restricted to inhibitory synapses in the spinal cord, brainstem and cerebellum (Chalphin & Saha, 2010; Muller, Le Corrionc, Triller, & Legendre, 2006).

The X-ray crystal structures of both of these transporters are not yet known. Homology modelling with the closely related eukaryotic dopamine transporters (DAT) or the prokaryotic leucine transporter (LeuT) has been used to predict

structural consequences of GlyT2 mutations (Penmatsa, Wang, & Gouaux, 2013; Wang, Penmatsa, & Gouaux, 2015; Yamashita, Singh, Kawate, Jin, & Gouaux, 2005). The transmembrane domain (TMD) presumably consists of 12 α -helices, with short intra- or extracellular loops connecting these TM helices. The N- and C-termini are localised intracellularly. TM helices 1-5 and TM helices 6-10 compose two structural motifs in opposite direction within both transmembrane segments. TM helix 1 and TM helix 6 constitute a break point in the middle of the TMD and are composed of two segments each (TM1a, TM1b, TM6a, TM6b). These two TM helices together with TM3 and TM8 represent the inner ring of the transporter which accommodates the substrate- and Na^+ -binding sites (Gomeza et al., 2003). The GlyT2 protein is transported as a glycosylated dimer or oligomer to the cellular membrane (Bartholomaeus et al., 2008; Fernandez-Sanchez, Diez-Guerra, Cubelos, Gimenez, & Zafra, 2008; Yamashita et al., 2005).

Sequencing of genomic DNA from patients with startle disease identified missense, frameshift and nonsense mutations distributed over the entire 16 exons of the *SLC6A5* gene (Rees et al., 2006). The majority of GlyT2 mutations in patients are compound heterozygous demonstrating single recessive mutations from the unaffected mother and father; however, when inherited together, they result in two affected *SLC6A5* alleles associated with a disease phenotype. In our study, we characterise the GlyT2 mutation P429L originally identified in an infant with startle disease homozygous for the DNA polymorphism c.1286C > T. Both parents were carriers of this polymorphism and harboured a second polymorphism c.1387G > A also located in exon 8. This second polymorphism was not identified in the affected infant. The family consists of two additional healthy children with the identical genotype compared with the parents (in exon 8) and two affected children homozygous for c.1286 C > T but negative for the second polymorphism c.1387 G > A (one child died at the age of 15 months). The mutation c.1286 C > T resulted in an amino acid exchange of a proline at amino acid position 429 into a leucine at the protein level. Our molecular characterisation identified lower whole cell expression accompanied by a loss of glycine transport. Homology modelling revealed that the exchange of the proline to leucine destroys the kink in the α -helix 5 produced by the proline and may affect the mobility of the adjacent α -helix 8, which mediates binding of sodium ions. Consequently, P429L is considered a loss of function mutation of GlyT2.

2 | MATERIALS AND METHODS

2.1 | Ethical statement

Experiments using patient material have been approved by the Ethics Committee of the Medical Faculty of the University

of Würzburg (No. 2019031201), Germany including permission granted by the family.

2.2 | Genomic DNA isolation

Genomic DNA (gDNA) was isolated from blood samples of human patients following the manufacturer's instructions using the DNA Blood Mini Kit (Qiagen, Hilden, Germany). Purified gDNA was stored at 4°C.

2.3 | Allele sequencing

To analyse the allelic distribution of the genomic mutations from different family members, exon 8 was amplified by PCR from the gDNA, cloned into a plasmid, and various clones were sequenced ($n = 10-12$).

2.4 | Site-directed mutagenesis

For generation of the GlyT2^{P429L} mutant, mutagenesis primers were redesigned (Life Technologies, Darmstadt, Germany): forward mutated primer 5'GGCCACGTTCCCTGTATGTCGACT3', reverse primer 5'GTACGACATACAGGAACGTGGCC3'. In addition, parental primers were designed including an additional restriction site to allow easy cloning (Cla I, Hind III): forward parental primer 5'TAG GTG ACA CTA TAG AAT AAC ATC3', reverse parental primer 5'GTA ACC ATT ATA AGC TGC AAT AAA CAA GTT3'. The first PCR generated two amplicons which overlapped in the region of the mutagenesis primer. Using both initial fragments in a second PCR as templates, two cycles without additional primer were run to let the 3'OH end of both strands be filled by the polymerase. Then, the two parental primers were added and the full length mutated GlyT2 was amplified in 28 additional PCR cycles. The PCR reaction contained 100 ng plasmid DNA (human GlyT2), 10 pmol of each primer, 5× HotStar HiFidelity PCR buffer (20 µl, included dNTPs), 1 µl of HotStar HiFidelity DNA Polymerase (2.5 U/µl, Qiagen, Hilden, Germany) and adjusted to 100 µl with sterile water. The PCR conditions were 5 min denaturation at 95°C, 5 min annealing at 50°C and 5 min elongation at 72°C. The final PCR product was cut with the newly introduced restriction sites for Hind III and Cla I and ligated into the mycGlyT2/pRK5 plasmid. The final construct was verified for the mutation by sequencing (LGC Genomics, Berlin, Germany).

2.5 | Cell lines

HEK293 cells (human embryonic kidney) were used for all *in vitro* experiments. The cell line was obtained from ATCC (CRL-1573; ATCC – Global Biosource Center, Manassas, VA, USA). HEK293 cells were grown in Minimum Essential Media (MEM, Life Technologies,

Darmstadt, Germany). The medium was supplemented with glutaMAX (200 mM) and sodium pyruvate (100 mM), penicillin (10,000 U/ml)/streptomycin (10,000 µg/ml) and 10% foetal calf serum. Cells were grown at 37°C and 5% CO₂. At a confluency of 75% (24 h after plating), cells were transfected using either the calcium phosphate precipitation method or lipofectamine. For calcium phosphate precipitation, cells were washed 6 h post-transfection and used either for immunocytochemical stainings and protein biochemical analysis 24–48 h after transfection. To perform glycine uptake assays, lipofectamin transfection of HEK293 cells was preferred.

COS7 cells were used for the compartmental analysis due to their large cytoplasm. Cells were obtained from ATCC (CRL-1651; ATCC – Global Biosource Center, Manassas, VA, USA). COS7 cells were transfected using dextran and PBS (phosphate-buffered saline) combined with plasmid DNA. Following 30 min at 37°C and 5% CO₂, cells were washed and incubated with chloroquine for an additional 2 h to increase transfection efficiency. After 2 h, chloroquine was washed away, and fresh medium was provided to the cells for another 48 h before cells were used for immunocytochemical stainings.

2.6 | Immunocytochemical stainings

Immunocytochemical stainings were performed from transfected HEK293 or COS7 cells. All stainings were done using permeabilized cells with Triton X-100. Cells grown on cover slips were washed with PBS pH 7.4 and fixed with 4% paraformaldehyde and 4% sucrose. Cells were washed three times with PBS and supplied to a blocking solution (PBS, 0.2% Triton X-100, 5% [v/v] normal goat serum) for 30 min at 21°C. Cells were then incubated with specific antibodies (myc epitope containing GlyT2 protein with the specific myc-antibody ab9106, Abcam, Cambridge, UK and A7 [TA100010, OriGene, Rockville, MD, USA], calnexin polyclonal rabbit antibody [1:200, ab22595, Abcam, Cambridge, UK], ERGIC53 mouse monoclonal antibody [1:250, Enzo Life Sciences, NYC, NY, USA]), and mouse monoclonal antibody GM130 (1:250, Franklin Lakes, NJ, USA). After additional washing, cells were incubated with secondary antibodies: goat anti-mouse Cy3 (1:250, Dianova, Hamburg, Germany) and goat anti-rabbit Alexa 488 (1:250, Dianova, Hamburg, Germany). DAPI staining of the nucleus was done in a 1:5,000 dilution in PBS for 5 min. Cells on cover slips were mounted on glass slides with mowiol. For the compartmental staining procedure, an additional quenching step was introduced after cell fixation using 50 mM NH₄Cl in PBS for 10 min. An Olympus microscope (Fluoview ix1000, Olympus, Hamburg, Germany) was utilised for image productions from stained transfected cells.

2.7 | Analysis of transfection capacities

GlyT2 wt and GlyT2^{P429L} were co-transfected with GFP plasmid and stained 48 h post-transfection. An Olympus IX81 microscope with Olympus FV1000 confocal laser scanning system was used to acquire fluorescence images. The FVD10 SPD spectral detector and diode lasers of 405 nm (DAPI), 495 nm (GFP) and 550 nm (Cy3) (Olympus, Tokyo, Japan) were used. Five images of three independent transfections (15 images total) and stainings were taken using Olympus UPLFLN 20× objective. Images were further processed, and cells were counted using ImageJ (1.52)/Fiji software (Schindelin et al., 2012). The number of DAPI-positive nuclei was used as total number of cells per image. The numbers of GFP and Cy3 positive cells (GlyT2 was stained with the monoclonal antibody anti-myc and the secondary goat anti-mouse Cy3 antibody) were calculated in percent dependent on the total amount of DAPI-positive cells. Mean values and SEM were calculated.

2.8 | Whole cell lysate and membrane preparation

Forty-eight hours post-transfection, whole cell lysates were obtained from transfected HEK293 cells using the protein extraction reagent CytoBuster (Novagen/Merck KGaA, Darmstadt, Germany). In brief, transfected cells from a 10 cm dish were washed once in PBS pH 7.4 and supplied with 500 µl CytoBuster reagent. Following 5 min incubation at 21°C, cells were collected by scraping them from the dish and centrifuged for 5 min at 4°C (16,000 g). Solubilised protein was located in the supernatant and stored at -80°C. For membrane protein analysis, crude cell membranes were prepared from cells transfected with either GlyT2 wt or GlyT2^{P429L} (Sontheimer et al., 1989).

2.9 | Endo H and PNGase F treatment

Endo H and PNGase F were used for deglycosylation experiments according to the manufacture's protocol (New England Biolabs, Ipswich, MA, USA).

2.10 | Glycine uptake assay

To perform the [³H]-glycine uptake assay, 96-well plates were gelatine coated. A total of 15,000 HEK293 cells were seeded per well and transfected 24 h after seeding with lipofectamine (Lipofectamine2000, Life Technologies, Darmstadt, Germany). Transfection with GFP served as MOCK control and to control of the transfection efficiency. Cells were either transfected with GlyT2 wild-type, GlyT2^{P429L} or defined ratios of 1:1 or 1:10 of both constructs (the total amount of plasmid was the same for

all conditions used). For the uptake assay, sterile-filtered HBS (HEPES-buffered saline) buffer pH 7.4 (5 mM KCl, 1 mM MgSO₄, HEPES-Tris, pH 7.4, 10 mM Glucose, 1 mM CaCl₂, 150 mM NaCl,) was used. The transport medium contained a concentration series of glycine. To reach final concentrations of glycine in a series of 0, 25, 50, 100, 250, 500, 750, 1000 µM, the [³H] glycine (stock 20.9 µM; 47.8 Ci/mmol, Perkin Elmer, Waltham, MA, USA) was used in a concentration series of 25, 50, 100, 250, 500, 750 and 1000 nM and supplied with 10 mM cold glycine to reach the final glycine concentrations (example: 1000 nM = 1 µM [³H] glycine was supplemented with 999 µM cold glycine to reach 1000 µM = 1 mM glycine in total) (Fornes, Nunez, Aragon, & Lopez-Corcuera, 2004; Gimenez et al., 2012). Cells were washed three times in HBS buffer and supplied with 80 µl of the appropriate transport medium with different glycine concentrations for 10 min at 37°C. All samples were done in triplicates. Cells were washed again three times with HBS buffer. Cell lysis was performed with 140 µl cold sterile H₂O for 10 min on ice. Lysed cells were homogenised. 100 µl were used for counting the amounts of glycine uptake. Counting was performed using the Perkin Elmer scintillation counter (Tri-Carb 2910TR, Perkin Elmer, Rodgau, Germany). 20 µl of lysate was used to determine the protein concentration in each probe, required for the calculation of the final uptake rate. Protein quantification was done using the Bradford assay (Bio Rad, Munich, Germany). The GFP-transfected cells refer to the endogenous transporter activity in HEK293 cells. There was no background correction done by subtracting these values from the GlyT2 transporter activities.

2.11 | Statistical data analysis

Western blots from whole cell protein fractions were quantified using the Image J software (NIH). GlyT2 protein bands were normalized to β-actin (housekeeping protein). Microcal Origin (Microcal Software, Inc.) was used to analyse the glycine uptake capability. The equation $y = v_{\max} * x^n / (K_m^n + x^n)$ was used to determine the maximal velocity (v_{\max}) of the uptake reaction as well as the half-maximal velocity referred to as K_m value. The graphs were generated using the Origin 6.0 software. Statistical data analysis was performed using Student's *t* test (analysis of variance) or one-way ANOVA. Significance values are represented with * $p \leq 0.05$, ** $p \leq 0.01$ and *** $p \leq 0.001$.

2.12 | Homology modelling and sequence alignment

The GlyT2 homology model was built with SWISS-MODEL (Arnold, Bordoli, Kopp, & Schwede, 2006) by

using the *Drosophila melanogaster* Dopamine transporter (DAT) (PDB:4XP4) (Wang et al., 2015) as the template model, which shares a sequence identity of ~49%. In silico site-directed mutagenesis was performed in COOT (Emsley & Cowtan, 2004) by taking into consideration clashes with surrounding residues while retaining proper stereochemistry of the mutated residues. Figures involving structural representation were prepared in PyMol (www.pymol.org). The multiple sequence alignment was performed by using Clustal omega (Sievers et al., 2011), and the representation was generated through the ESPript server (Robert & Gouet, 2014).

3 | RESULTS

3.1 | Patient description

The patient was the fourth child of two consanguineous parents, both were carriers of two polymorphisms in the coding region of the *SLC6A5* gene. The polymorphisms were located in exon 8 of the *SLC6A5* gene. Both parents (I/1 and I/2) were heterozygous for the determined polymorphisms c.1286 C > T and c.1387 G > A (Fig. 1a–c). At the protein level, the polymorphisms result in missense mutations of the encoded GlyT2 protein, P429L and D463N.

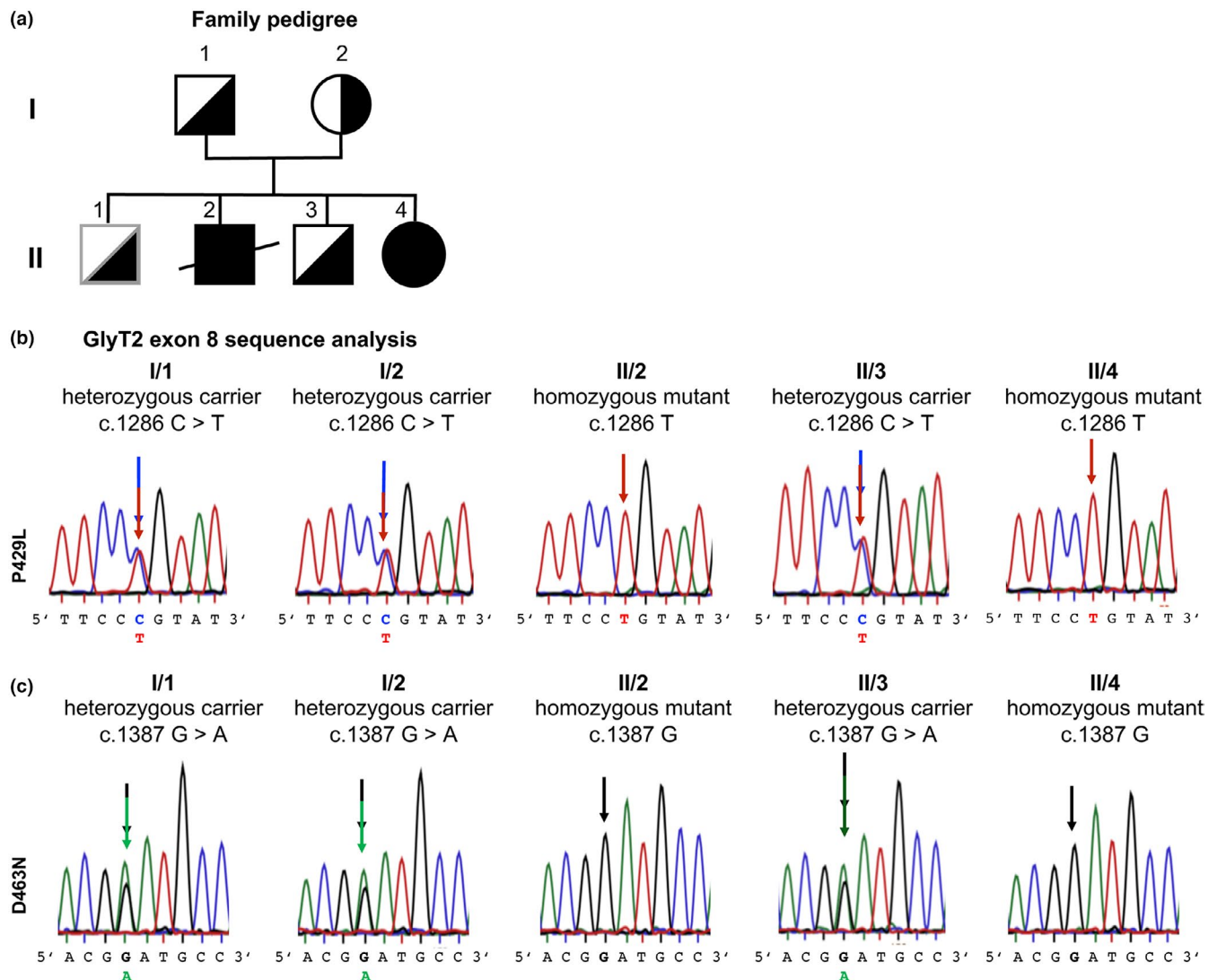


FIGURE 1 Overview about family pedigree and sequence analysis. (a) The family pedigree shows the two heterozygous parental carriers (generation I; I/1 and I/2) and their four children (generation II; II/1–4). Note, the genotype of child 1 (II/1, grey square) is not known due to a lack of material for sequencing analysis. (b,c) Sequence analysis of exon 8 amplified from genomic DNA. Both parents (I/1 and I/2) harbour two single nucleotide polymorphisms c.1286 C > T and c.1387 G > A localised in exon 8 of the *SLC6A5* gene and are therefore heterozygous carriers. Three children, two boys and one girl, were either heterozygous like the parents (II/3) or homozygous (II/2 and II/4) for the GlyT2 mutations. Child II/2 died at the age of 15 months and was homozygous for the c.1286 C > T (P429L at the protein level) mutation but did not carry the c.1387 G > A (D463N at the protein level) polymorphism. Child II/3 harbours both polymorphisms in a heterozygous configuration like the parents and is thus a heterozygous carrier for both DNA polymorphisms. Child II/4 is homozygous for c.1286 C > T but not a carrier of the second c.1387 G > A DNA polymorphism. [Colour figure can be viewed at wileyonlinelibrary.com]

Both GlyT2 variants are listed at the gnomAD database (P429L with only two allele counts out of 251140 alleles (no homozygous), frequency of 0.000008; and D463N with 63540 allele counts out of 282568 alleles (7954 homozygous), frequency of 0.22; <https://gnomad.broadinstitute.org/>). The original description of GlyT2 (*SLC6A5*) as presynaptic component of human hyperekplexia also identified the polymorphism c.1387 G > A (D463N) (Rees et al., 2006). The second child (II/2), a boy, was homozygous for P429L but did not harbour the mutation D463N (Fig. 1a–c). He died at the age of 15 months and suffered from severe hyperekplexia. The third child of the family (II/3) had the same genotype as the parents, representing a carrier of both mutations P429L and D463N (Fig. 1a–c). From the first child (II/1), no material for genotype analysis was available. Due to a lack of symptoms, we expect the same genotype as the parents (marked by the grey square in the pedigree Fig. 1a). The fourth child (II/4), a girl, had the same genotype as the second child (II/2) being homozygous at position c.1286 T (Fig. 1a–c). Again, severe symptoms of hyperekplexia were observed during the first weeks of life. This patient showed generalised stiffness after birth with an exaggerated startle response leading to stiffness with apnoea before treatment with clonazepam was started. At clinical examination, she demonstrated the typical exaggerated head retraction reflex, elicited by tapping her face, especially her chin. During the first year of life, she had repeated episodes of exaggerated startle that ameliorated with increasing doses of clonazepam. At the age of one year, she had mildly delayed developmental milestones and no further apnoeic spells.

3.2 | Single DNA polymorphisms are localised on different alleles

To investigate the allele distribution of the two identified polymorphisms, exon 8 was amplified from the genomic DNA of five family members and cloned into the plasmid pRK7 to separate DNA fragments from different alleles (Fig. 2a). From the sequencing data, we expected both mutations on different alleles in the parents (Fig. 2b). Single clones were sequenced, and the frequency of the polymorphisms quantified (Fig. 2c, Table 1). In all cases independent of parent or child, the cloned fragments contained only one of the polymorphisms which is in line with the presence of the two polymorphisms on different alleles. For homozygous patients, all clones contained c.1286 C > T. In contrast, c.1387 G > A was never observed in children suffered from hyperekplexia. The determined allele frequency for the heterozygous child (II/3) was similar to that of the parents (I/1 and I/2) (Fig. 2c, Table 1).

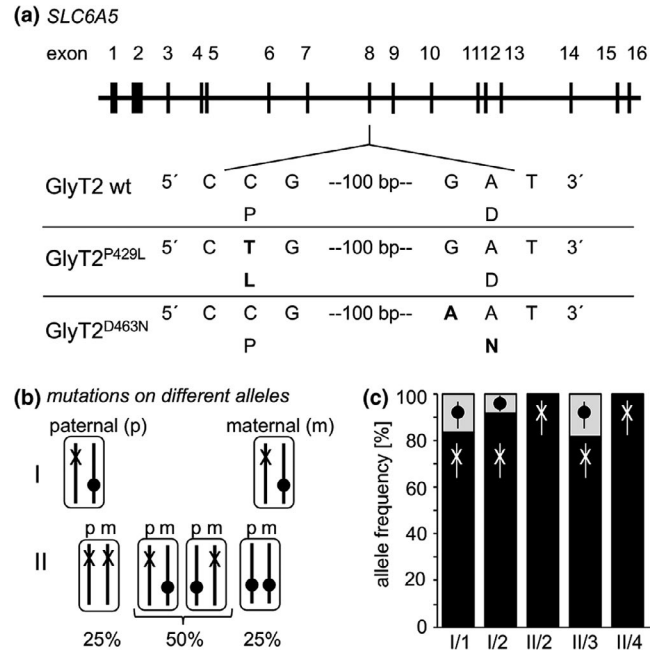


FIGURE 2 GlyT2 mutations in the parents are present on two alleles. (a) Allele frequency determined from amplification of exon 8 from five family members (I/1, I/2, II/2, II/3, II/4; except II/1 due to lack of material) followed by cloning and sequencing. (b) Scheme of allele distribution in case of two mutations present on different alleles in the parents (I, paternal and maternal). Mutations on different alleles are labelled with a cross or a circle (black filled). Possibilities of allele division in the second generation (II) with expected frequencies are shown. (c) Quantification of frequency of both mutations (P429L black bars labelled with cross and D463N grey marked with a black circle) from 10 to 12 clones. Note, each clone did always contain one mutation only, either c.1286 C > T (P429L) or c.1387 G > A (D463N)

3.3 | GlyT2^{P429L} shows trafficking through intracellular compartments

Following cloning of the mutation into the cDNA of GlyT2 wild type (wt), the GlyT2 variant P429L was transfected into HEK293 cells and analysed for cellular expression. To perform direct comparison between the GlyT2 wt and the GlyT2^{P429L} mutant, we analysed transfection capacity of both plasmids compared with co-transfected GFP. The co-transfected GFP as well as the constructs for GlyT2 wt and GlyT2^{P429L} exhibited similar transfection capacity (GlyT2 wt 25.4 ± 2.4% compared with GFP 26.7 ± 3%; GlyT2^{P429L} 22 ± 3% compared with GFP 28 ± 2.8%; Fig. 3a,b).

Cells were permeabilized to allow the GlyT2 antibody to reach the intracellular localised epitope. To discriminate between expression in the endoplasmic reticulum (ER) and at the plasma membrane (PM), plasmids encoding fusion proteins of pDsRed and the ER marker calreticulin or the plasma membrane marker GAP-43 were co-transfected. The GlyT2^{P429L} mutation did not hinder the protein from trafficking (Fig. 4). In co-transfected HEK293 cells, labelling was observed in

TABLE 1 Allele frequency obtained from human samples

Family member	GlyT2 P429L	Percentage (%)	GlyT2 D463N	Percentage (%)	<i>n</i>
I/1	10	83	2	17	12/12
I/2	11	92	1	8	12/12
II/2	10	100	0	0	10/10
II/3	9	82	2	18	11/12
II/4	10	100	0	0	10/10

n = samples with evaluable results/total samples analysed.

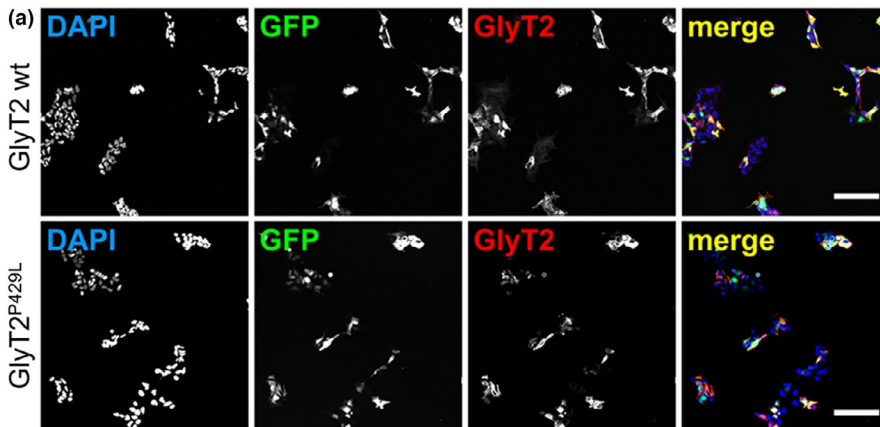
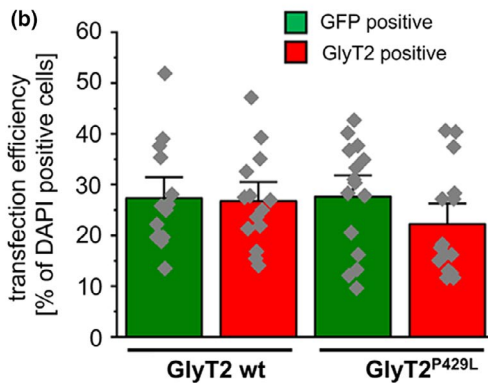


FIGURE 3 No differences in transfection capacity between GlyT2 wt and GlyT2 mutant. (a) GlyT2 and GlyT2^{P429L} (both in red) co-transfected with GFP (green) compared with the total number of DAPI-positive cells (blue = nuclear staining). Scale bar represents 100 μ m. (b) Quantification of transfection efficiencies for GlyT2 wt, and for the mutant GlyT2^{P429L}. [Colour figure can be viewed at wileyonlinelibrary.com]



the ER but also at the cellular membrane not obviously distinguishable from the GlyT2 wt protein (Fig. 4a,b). For trafficking analysis through different cellular compartments to the cellular surface, transfected COS7 cells were used. COS7 cells are more suitable for such an analysis due to their large cytoplasm. Similar to the experiments performed in HEK293 cells, GlyT2 wt or GlyT2^{P429L} was transfected with control plasmids labelling the ER (pDsRed-ER) or the plasma membrane (pDsRed-PM). Moreover, co-labelling with calnexin, an ER marker, ERGIC-53, a marker protein of the ER-Golgi intermediate compartment and GM130, a marker for the cis-Golgi compartment (Fig. 4c,d) resulted in co-localisation of those marker proteins together with either GlyT2 wt or GlyT2^{P429L}. In conclusion, the mutant as well as the wild-type GlyT2 protein was identified in compartments involved in protein trafficking.

Labelling at the cellular membrane was observed with less intensity for the mutant GlyT2^{P429L} compared with the GlyT2 wt (lower panels, Fig. 4c,d).

3.4 | The GlyT2 mutation results in a significant reduction of whole cell protein expression

The protein biochemical analysis of whole cell lysates from transfected HEK293 cells revealed expression of the GlyT2 wt and GlyT2^{P429L}. The GlyT2 antibody stained two protein bands at 100 kDa and 75 kDa. The whole cell protein amount obtained from cell lysates was significantly decreased for the mutant GlyT2^{P429L} compared with the GlyT2 wt protein ($51 \pm 10\%$, $p = 0.01$ compared with GlyT2 wt, Fig. 5a,b).

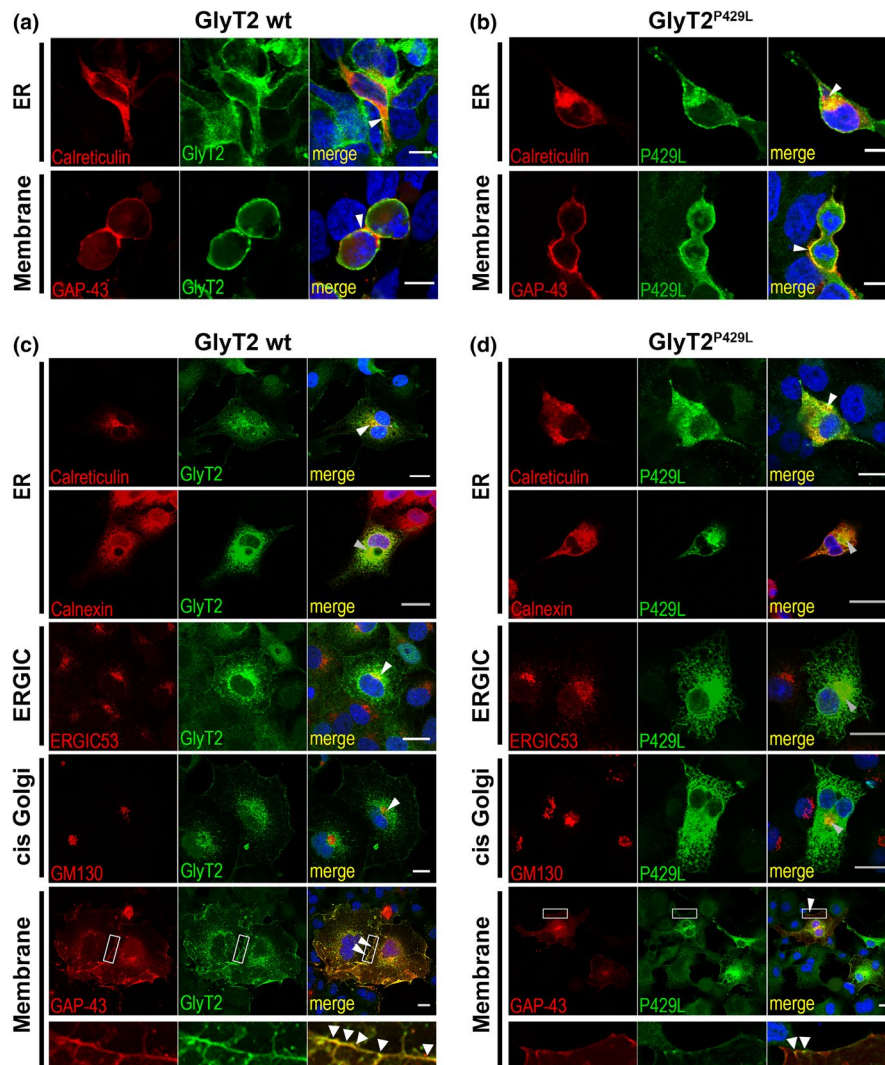


FIGURE 4 Cellular and compartmental analysis of the GlyT2^{P429L} mutant showed no general impairment compared with the wild-type protein. (a,b) GlyT2 wild type and the GlyT2^{P429L} variant were transfected into HEK293 cells and analysed for their cellular location. Cells were co-transfected with a plasmid coding for a fusion protein of pDsRed and calreticulin to label the ER or a fusion protein of pDsRed and GAP-43, a marker for the plasma membrane (PM). Cells were permeabilized due to binding of the myc-antibody to an intracellularly localised epitope. (a) GlyT2 wt expression in the ER (upper lane), and membrane expression (PM; lower lane) shown by the labelled ring at the membrane colocalizing with GAP-43. (b) The mutant GlyT2^{P429L} is expressed and colocalizes with the ER as well as with the membrane of transfected cells. White bar refers to 10 μ m. (c,d) Compartmental analysis to analyse the trafficking route of the wt and the mutant protein in transfected COS7 cells. The pDsRed calreticulin marker was co-transfected. The ER was also labelled with an antibody against calnexin (second lane). The ERGIC53 antibody was used to label the ER-Golgi intermediate compartment (ERGIC red, third lane). The Golgi apparatus was labelled (red) with a cis-Golgi marker GM130 (fourth lane). The last lane represents colocalization of the GlyT2 wt with the membrane marker GAP-43, which was co-transfected as a fusion protein with pDsRed. (Lowest lane) enlarged views of membrane colocalization. (d) Similar expression analysis of the GlyT2^{P429L} mutant in the ER (either calreticulin or calnexin co-staining), ERGIC = ER-Golgi intermediate compartment (ERGIC53), cis-Golgi (GM130) or PM (GAP-43). Right column in (c) and (d) represents the overlay of the green and red channels. White arrow heads point to colocalized proteins (yellow). White bar corresponds to 20 μ m. All staining experiments have been performed four times ($n = 4$, representative images are shown). [Colour figure can be viewed at wileyonlinelibrary.com]

An increase in the loaded protein led to an increase of the signal intensity for both the wt and the mutant protein, but the overall protein amount of GlyT2^{P429L} was consistently lower compared with the GlyT2 wt protein (Fig. 5c). The single quantification of the mature and immature proteins from the whole cell lysates revealed a significant reduction of GlyT2^{P429L} with $34 \pm 9\%$ ($p = 0.033$) of the GlyT2 wt for

the immature protein (75 kDa) and $61 \pm 9\%$ ($p = 0.006$) for the mature protein (100 kDa) (Fig. 5d). To verify that the mature band (100 kDa) is the glycosylated isoform and the immature protein (75 kDa) is non-glycosylated, membrane preparations obtained from GlyT2 wt and GlyT2^{P429L} transfected cells were used for digestion with endoglycosidases Endo H and PNGase F (Fig. 5e). PNGase F digestion removes

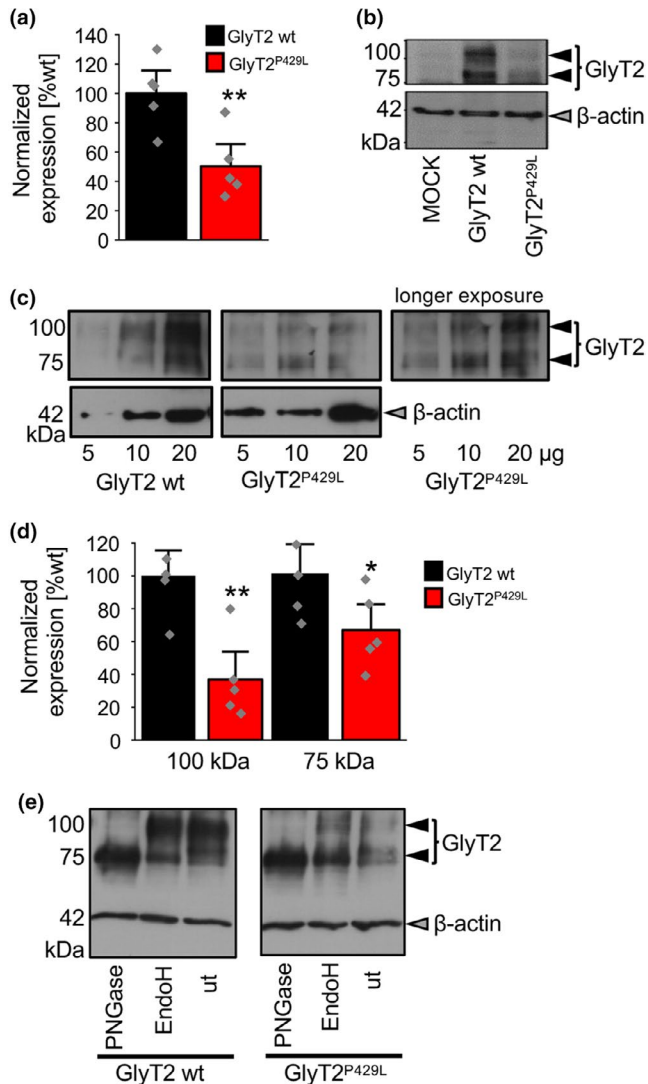


FIGURE 5 Whole cell expression differed between GlyT2 wild type (wt) and GlyT2^{P429L} mutant. (a) Quantification of whole cell GlyT2 wt and mutant protein from lysates normalised to β-actin (both bands were quantified together against β-actin protein amount); wt refers to 100%. (b) Representative gel demonstrating whole cell expression following transfection of GlyT2 wt and GlyT2^{P429L} into HEK293 cells. GFP plasmid was used for MOCK transfection allowing to control the transfection efficiency in parallel. β-Actin was used as housekeeping protein and stained to verify loading of the same protein amount. The GlyT2 antibody stained two protein bands (100 and 75 kDa). (c) Due to low protein amount determined for the mutant (see the comparison of low and long exposure times), the whole cell lysate was loaded at different protein amounts (5, 10, 20 μg) to the gel. β-Actin served as loading control. (d) Normalized expression of the mutant 100 and 75 kDa protein band to the wt protein (both bands for 100 and 75 kDa were quantified separately, values obtained for wt refer to 100% in each case). Significance values * $p \leq 0.05$, ** $p \leq 0.01$. (e) GlyT2 wt and GlyT2^{P429L} mutant were digested with endoglycosidases EndoH and PNGase F; non-digested control = ut (untreated). Note, the two bands reflect the mature (100 kDa) and immature (75 kDa) GlyT2 protein, respectively. [Colour figure can be viewed at wileyonlinelibrary.com]

mannose chains directly attached at asparagine. In contrast, Endo H cuts only high-mannose type glycans leaving only one *N*-acetylglucosamine attached at the asparagine until the Golgi α-glucosidase II cleaves off two mannose molecules. Both, GlyT2 wt and GlyT2^{P429L} were observed in the cis-Golgi compartment and thus possessed a higher sugar tree capable of being cut by PNGase F (Fig. 5e). Hence, we confirmed that the 100 kDa band refers to the mature GlyT2 and the immature (not fully glycosylated) GlyT2 protein is represented by the 75 kDa as has been reported earlier (Arribas-Gonzalez, de Juan-Sanz, Aragon, & Lopez-Corcuera, 2015; Gimenez et al., 2012).

3.5 | GlyT2^{P429L} is a loss of function mutation

The functional analysis of the GlyT2^{P429L} mutant was determined from glycine uptake assays. GFP transfection was used as negative control (5.0 ± 0.6 nmol/mg × min, refers to V_{max}) and represents the endogenous glycine transport of HEK293 cells as has been reported previously (Rees et al., 2006). The transfection efficiencies of GlyT2 wt and GlyT2^{P429L} together with GFP were similar (Fig. 6a). The glycine transport of GlyT2 wt showed a transport rate of 8.8 ± 0.5 nmol/mg × min (Fig. 6b, Table 2) which is comparable with previous reports. The GlyT2^{P429L} mutant lacked glycine transport and was indistinguishable from GFP-transfected cells serving as the negative control (at 250 μM glycine GlyT2^{P429L} 0.9 ± 0.1 nmol/mg × min; GFP control 1.4 ± 0.2 nmol/mg × min, non-significant $p = 0.39$; GlyT2 wt compared with GlyT2^{P429L} $p = 0.0007$, GlyT2 wt compared with GFP-transfected cells $p = 0.001$; Fig. 6b, Table 2). At all glycine concentrations, the GlyT2 wt revealed a significantly increased transport activity compared with the GlyT2^{P429L} mutant (Fig. 6b,c). To simulate *in vitro* situation in heterozygous human individuals, GlyT2 wt and GlyT2^{P429L} were expressed at a 1:1 ratio. The maximal transport activity obtained from the 1:1 wt : mutant expression was not significantly different from the GlyT2 wt expression alone with 6.9 ± 0.4 nmol/mg × min compared with 8.8 ± 0.5 nmol/mg × min for the wt situation ($p = 0.38$, Fig. 6b). The remaining transport activity (referring to the maximal transport activity) was $79 \pm 5\%$ of GlyT2 wt and explains the non-symptomatic phenotype of the heterozygous carriers. Using a 10-fold excess of GlyT2^{P429L} in coexpression with the wild type, the maximal transport activity was 5.5 ± 0.2 nmol/mg × min and thus not significantly different from the mutant GlyT2^{P429L} ($p = 0.41$, Fig. 6b, Table 2). The transport activity of the coexpressed GlyT2 wt and GlyT2^{P429L} mutant in a 1:10 ratio was, however, significantly reduced compared with GlyT2 wt alone ($p = 0.0008$, Fig. 6b, Table 2). Similar to the overall transport activity, the half-maximal transport activity

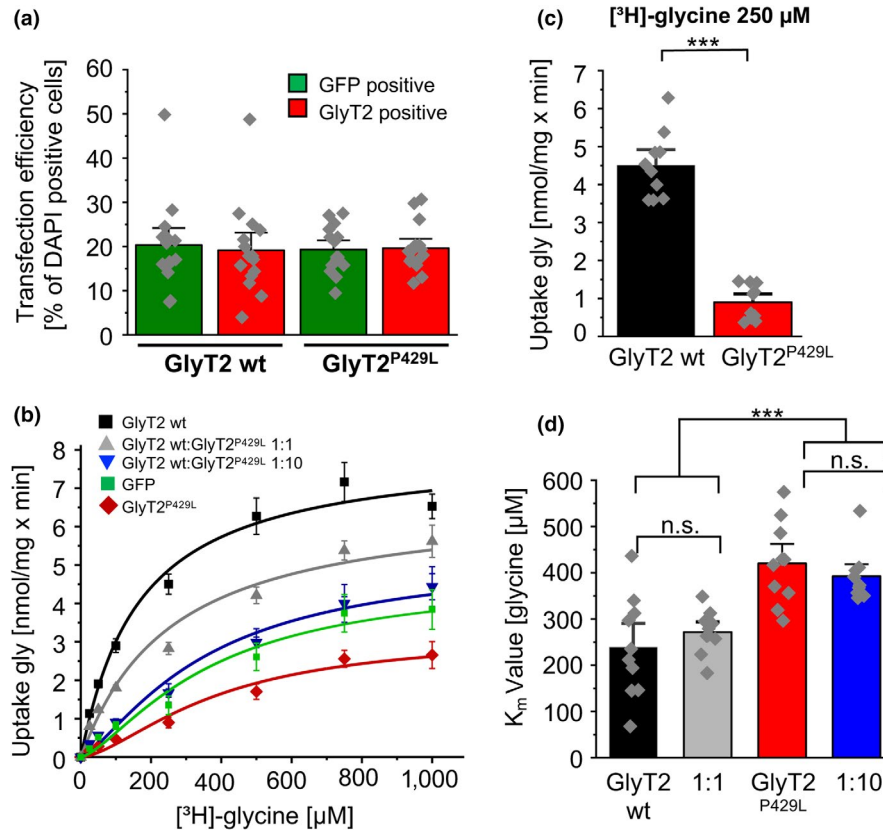


FIGURE 6 GlyT2^{P429L} is a loss of function mutation. The GlyT2 wt and the mutant GlyT2^{P429L} were transfected in 96-well plates. (a) GFP co-transfection revealed a similar transfection efficiency between the GlyT2 and the control GFP plasmid. (b) Glycine was applied in a concentration series (0, 10, 25, 100, 250, 500, 750, 1000 µM). Five independent experiments were performed; $n = 5$. Following lysis, glycine uptake was estimated in nmol/mg × min. GFP was used as MOCK control (green line), GlyT2 wt (black), GlyT2^{P429L} (red). GlyT2 wt and GlyT2^{P429L} were transfected in different ratios (1:1 GlyT2 wt : GlyT2^{P429L}, grey; 1:10 GlyT2 wt : GlyT2^{P429L}, blue). Note, the GFP-transfected cells refer to the endogenous transporter activity in HEK293 cells. The values between GFP and GlyT2^{P429L} were however not significantly different. No background correction was done by subtracting these values from the GlyT2 transporter activities. (c) Quantification of glycine uptake at 250 µM glycine, comparison of GlyT2 wt (black) and GlyT2^{P429L} (red) is shown. (d) Half-maximal velocity $V_{max}/2$ refers to the K_m value. The glycine concentration at the half-maximal velocity is compared between GlyT2 wt (black), GlyT2^{P429L} mutant (red) and different ratios 1:1 (grey), 1:10 (blue). Significance values $**p \leq 0.01$, $***p \leq 0.001$. n.s. = non-significant. [Colour figure can be viewed at wileyonlinelibrary.com]

TABLE 2 Glycine uptake kinetic parameters

Glycine (µM)	GFP	GlyT2 wt uptake [nmol/mg × min]	GlyT2 wt: GlyT2P429L 1:1 uptake [nmol/mg × min]	GlyT2 ^{P429L} uptake [nmol/mg × min]	GlyT2 wt: GlyT2P429L 1:10 uptake [nmol/mg × min]
0	0	0	0	0	0
25	0.2 ± 0.03	1.1 ± 0.1	0.8 ± 0.04	0.2 ± 0.03	0.4 ± 0.01
50	0.5 ± 0.04	1.9 ± 0.1	1.2 ± 0.1	0.3 ± 0.05	0.6 ± 0.03
100	0.8 ± 0.1	2.9 ± 0.2	1.8 ± 0.1	0.5 ± 0.1	0.9 ± 0.03
250	1.4 ± 0.2	4.5 ± 0.3	2.8 ± 0.2	0.9 ± 0.1	1.7 ± 0.1
500	2.6 ± 0.4	6.3 ± 0.5	4.2 ± 0.2	1.7 ± 0.2	3.0 ± 0.1
750	3.7 ± 0.5	7.2 ± 0.5	5.4 ± 0.3	2.6 ± 0.2	4.0 ± 0.2
1000	3.8 ± 0.5	6.5 ± 0.3	5.6 ± 0.4	2.7 ± 0.4	4.4 ± 0.3
$k_m = v_{max}/2$ at glycine (µM)	431 ± 28	239 ± 33	272 ± 14	420 ± 27	393 ± 16
v_{max} (nmol/mg × min)	5.0 ± 0.6	8.8 ± 0.5	6.9 ± 0.4	3.2 ± 0.3	5.5 ± 0.2

was reached at significantly lower glycine concentrations for the GlyT2 wt ($239 \pm 33 \mu\text{M}$) compared with GlyT2^{P429L} ($420 \pm 27 \mu\text{M}$), and the 1:10 ratio of the GlyT2 wt and GlyT2^{P429L} (1:10 ratio $393 \pm 16 \mu\text{M}$) but not different to the 1:1 ratio of wt and mutant (1:1 ratio $272 \pm 14 \mu\text{M}$, Fig. 6d, Table 2). Hence, 50% of mutated GlyT2 protein does not lead to major changes in the transporter activity; however, 10% of the GlyT2 wt drives the decrease in glycine transport towards lower substrate affinity comparable with the situation in the mutant GlyT2^{P429L}. Together with the expression analysis, these data reflect that the non-functionality of the mutant GlyT2^{P429L} is attributed to significantly reduced whole cell GlyT2^{P429L} protein which lacks glycine transport activity.

3.6 | Structural basis for the GlyT2 mutation

To gain insights into the effect of mutations at the structural level, a homology model of GlyT2 was built and both mutations were mapped onto the structure (Fig. 7a). P429, the site of the P429L mutation resides in α -helix 5 and the second mutation site D463N maps to the loop, which precedes α -helix 6. The *in silico* mutational analysis suggests that the P429L mutation would not only destroy the kink in the helix produced by the proline but might also affect the mobility of the adjacent α -helix 8. Interestingly, α -helix 8 in the GlyT2 model, corresponding to α -helix-8 in the case of the *Drosophila melanogaster* DAT structure (Penmatsa et al., 2013) mediates binding of a sodium ion (Na^+). Hence, the altered mobility could potentially play a pivotal role in the gating mechanisms of the transporter. Thus, the P429L mutation can most likely be associated with a sub-optimal functionality of the transporter (Fig. 7b,c). Interestingly, a multiple sequence alignment of human GlyT2, *Drosophila melanogaster* DAT and prokaryotic LeuT revealed that P429 is conserved in both eukaryotic transporters (Fig. 7f). Inspection of D463 revealed that this residue forms a salt-bridge with K460 located in the short helix at the extracellular region (Fig. 7d,e). The mutation D463N would abolish this salt-bridge while still leaving the ability to form a hydrogen bond.

4 | DISCUSSION

In this paper, we characterise the pathomechanism of a novel GlyT2 mutation at the molecular, cellular and protein levels generating severe hyperekplexia in affected homozygous individuals. Several reports have shown that mutations in GlyT2 are the second most common source for the neurological disorder startle disease (hyperekplexia) (Carta et al., 2012; Eulenburg et al., 2005; Harvey et al., 2008). Most mutations in GlyT2 identified so far are recessive ranging from missense mutations, frameshift mutations, nonsense or

splice site mutations (Carta et al., 2012). In addition to recessive mutants, two dominant negative mutations, Y705C and S512R, were described associated with impaired transporter trafficking and trapping of mutated GlyT2 by calnexin resulting in ER retention (Arribas-Gonzalez et al., 2015; Gimenez et al., 2012). In contrast, recessive missense mutations have not been shown to exhibit disturbed protein transport (Rees et al., 2006). Here, we identified a novel recessive mutation P429L in exon 8 of GlyT2 in a large family with both parents being carriers of two polymorphisms c.1286 C > T and c.1387 G > A. The family had four children, two suffered from startle disease and two unaffected children. Interestingly, the second polymorphism c.1387 G > A was present also in the unaffected children but never found in the affected children. Thus, we hypothesised that each polymorphism is present on only one allele in the parents as well as the unaffected children. Indeed, we found allelism for both DNA polymorphisms. In case of the two children suffering from startle disease, the polymorphism c.1286 C > T was found homozygous with both alleles affected. The second polymorphism was never detected in the affected individuals when c.1286 C > T was present on both alleles. One child carrying the GlyT2^{P429L} mutation died at the age of 15 months, the second affected child is being treated with clonazepam, which is usually used as symptomatic treatment. Although the mechanism of clonazepam in this regard is unknown, it is believed that an enhancement of GABAergic inhibition rescues the lack or impairment of the glycinergic inhibition (Andermann, Keene, Andermann, & Quesney, 1980).

Due to the severe effect of the mutation GlyT2^{P429L} in the patient, we setup an experimental series to describe the underlying pathology at the molecular, cellular and functional level. The protein trafficking route was followed through various cellular compartments involved in membrane protein forward transport (Schaefer et al., 2015; Valkova et al., 2011). Usually, ER membrane-bound protein is detectable during polypeptide synthesis (Park & Rapoport, 2012). Furthermore, it was previously shown that GlyT2 glycosylation and interaction with ER chaperones stabilize correct folding and facilitate transporter processing (Arribas-Gonzalez, Alonso-Torres, Aragon, & Lopez-Corcuera, 2013; Martinez-Maza et al., 2001; Rutkevich & Williams, 2011). The subcellular analysis revealed a positive staining of the mutant GlyT2^{P429L} in the ER colocalized with calreticulin and calnexin, but also with ERGIC53 in the ER-Golgi intermediate compartment and GM130 in the cis-Golgi arguing for ER export of the GlyT2^{P429L} mutant. Arribas-Gonzalez et al. (2015) reported enhanced accumulation trapped to calnexin for the dominant mutant GlyT2^{S521R}. Colocalization of GlyT2^{P429L} with the ER chaperone calnexin as well as detection of the mutant in cellular compartments downstream of the ER and finally surface integration argue for no obvious trafficking defect of the mutant. However, it cannot be

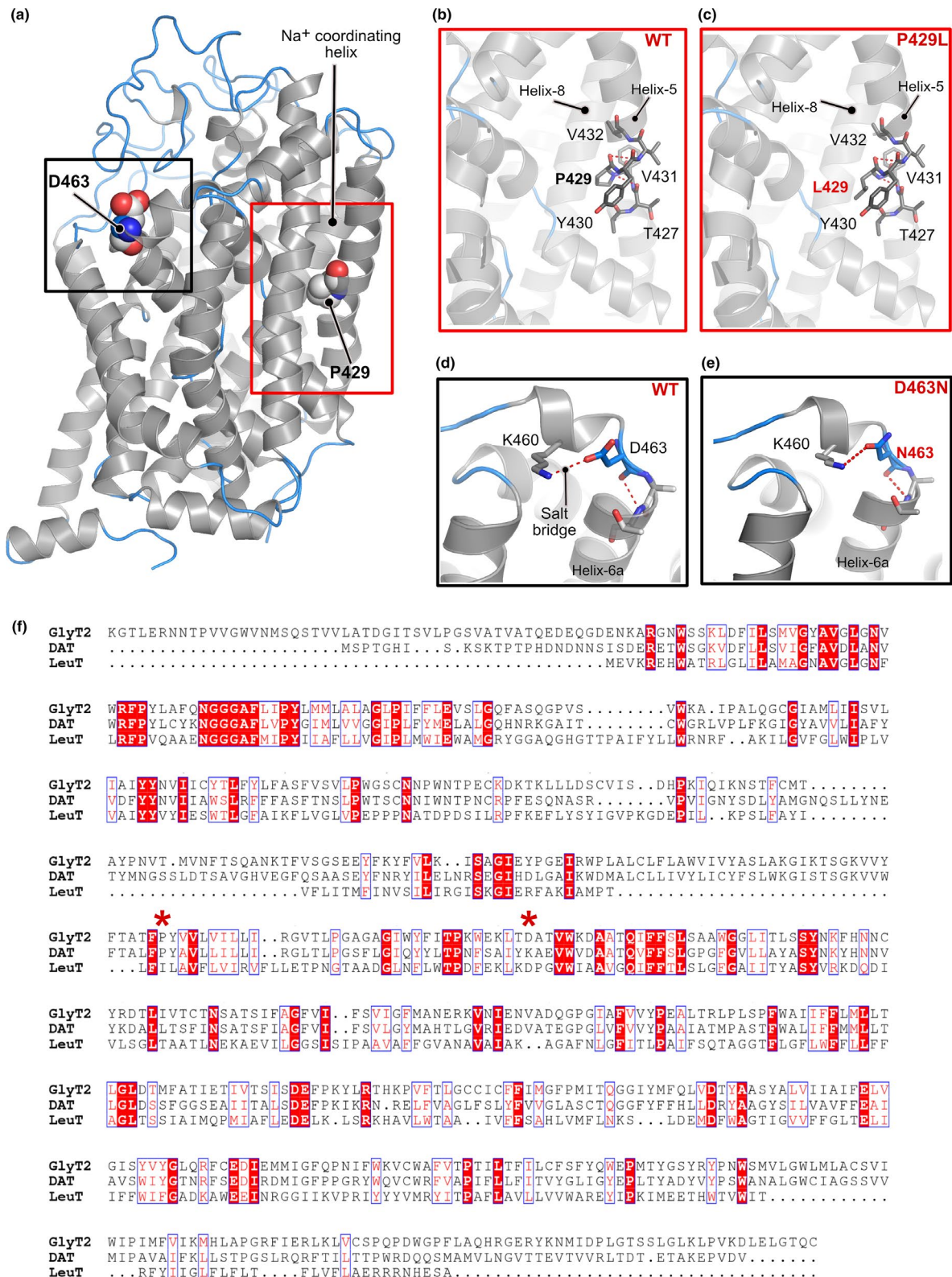


FIGURE 7 Structural basis for the GlyT2 mutation. (a) Cartoon representation of the overall architecture of the GlyT2 model with the helices is coloured in grey and the loops in blue. The residues which account for the mutations are displayed in space-filling representation. The helices are numbered according to the *Drosophila melanogaster* DAT structure. (b,c) Enlarged views of the P429 and the mutant L429 with the residues interacting with P/L429 displayed in stick representation. (d,e) Enlarged views of D463 and the N463 mutant, which disrupt the salt-bridge between D463 and K460 (d). Critical residues are shown in stick representation. (f) Multiple sequence alignment of human GlyT2, *Drosophila* DAT and bacterial LeuT generated with the ESPrnt server. Sites of the mutations are shown with asterisks. [Colour figure can be viewed at wileyonlinelibrary.com]

excluded that the accumulation with the ER protein calnexin comprises trapping of the GlyT2^{P429L} protein to some extent which might lead to a migratory defect of the mutated transporter. To further corroborate the GlyT2^{P429L} mutant protein expression, the whole cell protein of GlyT2 in cell lysates was investigated. GlyT2 was always stained in two protein bands at the respective molecular weights 75 (immature) and 100 (mature) kDa (Arribas-Gonzalez et al., 2015; Gimenez et al., 2012). Cell lysate preparations clearly demonstrated that the general protein expression of the mutant GlyT2^{P429L} was significantly reduced compared with the wild-type transporter protein. The quantification exhibited around 50% less protein expression. Although the reduced protein expression most probably contributed to the observed disease phenotype in the affected children, a 50% reduction of the mature protein should be sufficient to fulfil the glycine recycling function of the glycine transporter (Carta et al., 2012; Rees et al., 2006). Moreover, GlyT2^{P429L} was also identified in membranes at the cellular surface. This is in contrast to the dominant negative mutant GlyT2^{S512R} which showed a complete absence from the cellular surface (Arribas-Gonzalez et al., 2015).

The functional analysis revealed that the mutated protein present at the cellular surface is not capable of transporting the neurotransmitter glycine. The observed transport rate for glycine was indistinguishable from MOCK-transfected cells. The glycine transport efficacy of the GlyT2 wild-type protein was similar to that from other reports in the literature (transport rates between 38–43 nmol/mg × 5 min) (Arribas-Gonzalez et al., 2015; Gimenez et al., 2012; Rees et al., 2006). Since the mutation is recessive, we expected to rescue the transport activity by coexpression with the GlyT2 wild-type protein in a 1:1 ratio (Rees et al., 2006). Indeed, coexpression of GlyT2 wild-type with the mutant in a 1:1 ratio showed no significant difference in the glycine transport activity pattern. This observation matches the symptomless phenotype of the parents whose GlyT2 expression pattern is reflected by a 1:1 ratio of GlyT2 wild-type and mutant protein. Hence, the heterozygous parents and unaffected children sharing the same genotype do not resemble any clinical symptoms of startle disease due to sufficient glycine recycling to enable proper inhibitory neurotransmission. These data clearly demonstrate that the mutation GlyT2^{P429L} follows a recessive trait which can be rescued by coexpressed wild-type transporter.

An increase in the amount of the mutant protein (90% of mutant GlyT2^{P429L} protein compared with wild-type protein 10%) shifted the transport activity to lower affinities as observed for GlyT2^{P429L} suggesting that the loss of function is mostly responsible for the disease pathology. Thus, the presence of two affected alleles resulted in a 51% decrease of the general protein expression, but the remaining GlyT2^{P429L} transporter lacked protein function.

Finally, we used homology modelling using the *Drosophila melanogaster* DAT transporter (Penmatsa et al., 2013; Wang et al., 2015) as a template to support the experimental data by identifying possible changes in the structure of the transporter. The location of the GlyT2 mutation P429L in α -helix 5 most probably destroyed the kink in this helix produced by the proline. As a consequence, the mobility of the adjacent α -helix 8 may be impaired. In the structure of the DAT transporter, the location of the P429L mutation is also in α -helix 8 (Penmatsa et al., 2013). In addition to a possible disruption of the α -helical structure of α -helix 5, the amino acid position P429 is close to the sodium-binding site. Hence, the mutation P429L might also affect the gating mechanism of the transporter. In contrast, *in silico* analysis of the second mutation D463N predicts the loss of a salt-bridge but leaves the ability to form a hydrogen bond. These data are in line with the observed high frequency of the c.1387 G>A polymorphism (D463N at the protein level) in the normal healthy population.

In conclusion, our data expand the current view of the GlyT2 pathology with the identification of a novel missense mutation P429L (homozygous) located in α -helix 5 from a patient with severe startle disease resulting in perturbed glycine recycling and thus a blockade of glycinergic inhibition.

ACKNOWLEDGEMENTS

Nadine Vornberger and Dana Wegmann are greatly acknowledged for their excellent technical assistance. We would like to thank Sylvia Hengst from the Rudolf Virchow Center for Experimental Biomedicine, University of Würzburg for her assistance with the scintillation counting. We are grateful to Rob Harvey who provided the GFP-tagged GlyT2/pRK5 and myc-tagged GlyT2/pRK5 plasmids. This work was supported by DFG VI586 (C.V.). N.S. was supported by the Scientia Program of the University of Würzburg.

CONFLICT OF INTEREST

The authors declare no competing financial interests.

DATA AVAILABILITY

Data are available on request by the authors.

AUTHOR CONTRIBUTIONS

A.K. and N.S. conducted mutagenesis. T.P. and R.H. recruited the patient material. A.K. and N.S. performed cell line transfections and immunocytochemical stainings. A.K. and N.S. analysed the expression data. A.K., C.V. conducted the glycine uptake assay. V.B.K. and H.S. performed GlyT2 homology modelling. A.K., N.S., V.B.K., T.P. performed data analyses. C.V. developed the study design. C.V.,

V.B.K., H.S., A.K., T.P. participated in manuscript writing. C.V. initiated, designed and supervised the project and wrote the manuscript.

ORCID

Carmen Villmann  <https://orcid.org/0000-0003-1498-6950>

REFERENCES

- Andermann, F., Keene, D. L., Andermann, E., & Quesney, L. F. (1980). Startle disease or hyperekplexia: Further delineation of the syndrome. *Brain*, *103*, 985–997.
- Arnold, K., Bordoli, L., Kopp, J., & Schwede, T. (2006). The SWISS-MODEL workspace: A web-based environment for protein structure homology modelling. *Bioinformatics*, *22*, 195–201.
- Arribas-Gonzalez, E., Alonso-Torres, P., Aragon, C., & Lopez-Corcuera, B. (2013). Calnexin-assisted biogenesis of the neuronal glycine transporter 2 (GlyT2). *PLoS ONE*, *8*, e63230.
- Arribas-Gonzalez, E., de Juan-Sanz, J., Aragon, C., & Lopez-Corcuera, B. (2015). Molecular basis of the dominant negative effect of a glycine transporter 2 mutation associated with hyperekplexia. *Journal of Biological Chemistry*, *290*, 2150–2165.
- Bartholomaus, I., Milan-Lobo, L., Nicke, A., Dutertre, S., Hastrup, H., Jha, A., ... Eulenburg, V. (2008). Glycine transporter dimers: Evidence for occurrence in the plasma membrane. *Journal of Biological Chemistry*, *283*, 10978–10991.
- Bode, A., & Lynch, J. W. (2014). The impact of human hyperekplexia mutations on glycine receptor structure and function. *Molecular Brain*, *7*, 2.
- Busselberg, D., Bischoff, A. M., Paton, J. F., & Richter, D. W. (2001). Reorganisation of respiratory network activity after loss of glycinergic inhibition. *Pflugers Archiv: European Journal of Physiology*, *441*, 444–449.
- Carta, E., Chung, S. K., James, V. M., Robinson, A., Gill, J. L., Remy, N., ... Harvey, R. J. (2012). Mutations in the GlyT2 gene (SLC6A5) are a second major cause of startle disease. *Journal of Biological Chemistry*, *287*, 28975–28985.
- Chalphin, A. V., & Saha, M. S. (2010). The specification of glycinergic neurons and the role of glycinergic transmission in development. *Frontiers in Molecular Neuroscience*, *3*, 11.
- Emsley, P., & Cowtan, K. (2004). Coot: Model-building tools for molecular graphics. *Acta Crystallographica. Section D, Biological Crystallography*, *60*, 2126–2132.
- Eulenburg, V., Armsen, W., Betz, H., & Gomeza, J. (2005). Glycine transporters: Essential regulators of neurotransmission. *Trends in Biochemical Sciences*, *30*, 325–333.
- Eulenburg, V., Becker, K., Gomeza, J., Schmitt, B., Becker, C. M., & Betz, H. (2006). Mutations within the human GLYT2 (SLC6A5) gene associated with hyperekplexia. *Biochemical and Biophysical Research Communications*, *348*, 400–405.
- Fernandez-Sanchez, E., Diez-Guerra, F. J., Cubelos, B., Gimenez, C., & Zafra, F. (2008). Mechanisms of endoplasmic-reticulum export of glycine transporter-1 (GLYT1). *The Biochemical Journal*, *409*, 669–681.
- Fornes, A., Nunez, E., Aragon, C., & Lopez-Corcuera, B. (2004). The second intracellular loop of the glycine transporter 2 contains crucial residues for glycine transport and phorbol ester-induced regulation. *Journal of Biological Chemistry*, *279*, 22934–22943.
- Gimenez, C., Perez-Siles, G., Martinez-Villarreal, J., Arribas-Gonzalez, E., Jimenez, E., Nunez, E., ... Lopez-Corcuera, B. (2012). A novel dominant hyperekplexia mutation Y705C alters trafficking and biochemical properties of the presynaptic glycine transporter GlyT2. *Journal of Biological Chemistry*, *287*, 28986–29002.
- Gomeza, J., Ohno, K., Hulsmann, S., Armsen, W., Eulenburg, V., Richter, D. W., ... Betz, H. (2003). Deletion of the mouse glycine transporter 2 results in a hyperekplexia phenotype and postnatal lethality. *Neuron*, *40*, 797–806.
- Harvey, R. J., Topf, M., Harvey, K., & Rees, M. I. (2008). The genetics of hyperekplexia: More than startle!. *Trends in Genetics*, *24*, 439–447.
- Harvey, R. J., & Yee, B. K. (2013). Glycine transporters as novel therapeutic targets in schizophrenia, alcohol dependence and pain. *Nature Reviews. Drug Discovery*, *12*, 866–885.
- Hulsmann, S., Oke, Y., Mesuret, G., Latal, A. T., Fortuna, M. G., Niebert, M., ... Hammerschmidt, K. (2019). The postnatal development of ultrasonic vocalization-associated breathing is altered in glycine transporter 2-deficient mice. *Journal of Physiology*, *597*, 173–191.
- Martinez-Maza, R., Poyatos, I., Lopez-Corcuera, B., Núñez, E., Gimenez, C., Zafra, F., & Aragon, C. (2001). The role of N-glycosylation in transport to the plasma membrane and sorting of the neuronal glycine transporter GLYT2. *Journal of Biological Chemistry*, *276*, 2168–2173.
- Masri, A., Chung, S. K., & Rees, M. I. (2017). Hyperekplexia: Report on phenotype and genotype of 16 Jordanian patients. *Brain & Development*, *39*, 306–311.
- Muller, E., Le Corronec, H., Triller, A., & Legendre, P. (2006). Developmental dissociation of presynaptic inhibitory neurotransmitter and postsynaptic receptor clustering in the hypoglossal nucleus. *Molecular and Cellular Neurosciences*, *32*, 254–273.
- Nigro, M. A., & Lim, H. C. (1992). Hyperekplexia and sudden neonatal death. *Pediatric Neurology*, *8*, 221–225.
- Park, E., & Rapoport, T. A. (2012). Mechanisms of Sec61/SecY-mediated protein translocation across membranes. *Annual Review of Biophysics*, *41*, 21–40.
- Penmatsa, A., Wang, K. H., & Gouaux, E. (2013). X-ray structure of dopamine transporter elucidates antidepressant mechanism. *Nature*, *503*, 85–90.
- Perez-Siles, G., Nunez, E., Morreale, A., Jimenez, E., Leo-Macias, A., Pita, G., ... Lopez-Corcuera, B. (2012). An aspartate residue in the external vestibule of GLYT2 (glycine transporter 2) controls cation access and transport coupling. *The Biochemical Journal*, *442*, 323–334.
- Rees, M. I., Harvey, K., Pearce, B. R., Chung, S. K., Duguid, I. C., Thomas, P., ... Harvey, R. J. (2006). Mutations in the gene encoding GlyT2 (SLC6A5) define a presynaptic component of human startle disease. *Nature Genetics*, *38*, 801–806.
- Robert, X., & Gouet, P. (2014). Deciphering key features in protein structures with the new ENDSript server. *Nucleic Acids Research*, *42*, W320–W324.
- Roux, M. J., & Supplisson, S. (2000). Neuronal and glial glycine transporters have different stoichiometries. *Neuron*, *25*, 373–383.
- Rutkevich, L. A., & Williams, D. B. (2011). Participation of lectin chaperones and thiol oxidoreductases in protein folding within

- the endoplasmic reticulum. *Current Opinion in Cell Biology*, 23, 157–166.
- Schaefer, N., Kluck, C. J., Price, K. L., Meiselbach, H., Vornberger, N., Schwarzinger, S., ... Villmann, C. (2015). Disturbed neuronal ER-golgi sorting of unassembled glycine receptors suggests altered subcellular processing is a cause of human hyperekplexia. *Journal of Neuroscience*, 35, 422–437.
- Schaefer, N., Roemer, V., Janzen, D., & Villmann, C. (2018). Impaired glycine receptor trafficking in neurological diseases. *Frontiers in Molecular Neuroscience*, 11, 291.
- Schindelin, J., Arganda-Carreras, I., Frise, E., Kaynig, V., Longair, M., Pietzsch, T., ... Cardona, A. (2012). Fiji: An open-source platform for biological-image analysis. *Nature Methods*, 9, 676–682.
- Shevtsova, N. A., Busselberg, D., Molkov, Y. I., Bischoff, A. M., Smith, J. C., Richter, D. W., & Rybak, I. A. (2014). Effects of glycinergic inhibition failure on respiratory rhythm and pattern generation. *Progress in Brain Research*, 209, 25–38.
- Sievers, F., Wilm, A., Dineen, D., Gibson, T. J., Karplus, K., Li, W., ... Higgins, D. G. (2011). Fast, scalable generation of high-quality protein multiple sequence alignments using Clustal Omega. *Molecular Systems Biology*, 7, 539.
- Sontheimer, H., Becker, C. M., Pritchett, D. B., Schofield, P. R., Grenningloh, G., Kettenmann, H., ... Seeburg, P. H. (1989). Functional chloride channels by mammalian cell expression of rat glycine receptor subunit. *Neuron*, 2, 1491–1497.
- Supplisson, S., & Roux, M. J. (2002). Why glycine transporters have different stoichiometries. *FEBS Letters*, 529, 93–101.
- Thomas, R. H., Chung, S. K., Wood, S. E., Cushion, T. D., Drew, C. J., Hammond, C. L., ... Rees, M. I. (2013). Genotype-phenotype correlations in hyperekplexia: Apnoeas, learning difficulties and speech delay. *Brain*, 136, 3085–3095.
- Valkova, C., Albrizio, M., Roder, I. V., Schwake, M., Betto, R., Rudolf, R., & Kaether, C. (2011). Sorting receptor Rer1 controls surface expression of muscle acetylcholine receptors by ER retention of unassembled alpha-subunits. *Proceedings of the National Academy of Sciences of the United States of America*, 108, 621–625.
- Vigevano, F., Di Capua, M., & Dalla Bernardina, B. (1989). Startle disease: An avoidable cause of sudden infant death. *Lancet*, 1, 216.
- Wang, K. H., Penmatsa, A., & Gouaux, E. (2015). Neurotransmitter and psychostimulant recognition by the dopamine transporter. *Nature*, 521, 322–327.
- Yamashita, A., Singh, S. K., Kawate, T., Jin, Y., & Gouaux, E. (2005). Crystal structure of a bacterial homologue of Na⁺/Cl⁻-dependent neurotransmitter transporters. *Nature*, 437, 215–223.
- Zafra, F., Aragon, C., Olivares, L., Danbolt, N. C., Gimenez, C., & Storm-Mathisen, J. (1995). Glycine transporters are differentially expressed among CNS cells. *Journal of Neuroscience*, 15, 3952–3969.

How to cite this article: Kitzenmaier A, Schaefer N, Kasaragod VB, et al. The P429L loss of function mutation of the human glycine transporter 2 associated with hyperekplexia. *Eur J Neurosci*. 2019;50:3906–3920. <https://doi.org/10.1111/ejn.14533>